J. Biochem. 122, 55-63 (1997)

Enzyme Flexibility: A New Concept in Recognition of Hydrophobic Substrates[1]

Shin-ichi Kawaguchi,*[,3] Yuko Nobe,* Jun-ichi Yasuoka,† Tateaki Wakamiya,†[,2] Shoichi Kusumoto,† and Seiki Kuramitsu*[,4]

*Department of Biology and †Department of Chemistry, Graduate School of Science, Osaka University, Toyonaka, Osaka 560

Received for publication, January 20, 1997

The mechanism of recognition of hydrophobic substrates was investigated using *Escherichia coli* aspartate aminotransferase (AspAT), *E. coli* aromatic amino acid aminotransferase (AroAT), and their chimeric enzyme (DY18). Surprisingly, broad substrate specificity was observed in the reaction of aminotransferases with hydrophobic substrates. The catalytic efficiency increased with an increase in the side chain length of straight or branched-terminal aliphatic substrates. The straight-chain substrates catalysed with maximal efficiency were the 7-carbon substrate in the case of AspAT and the 8-carbon substrate for AroAT and DY18. Consecutive addition of single methylene groups to the substrate had a constant effect on the stabilization energy of the transition state relative to the unbound state. The dependency of binding energy on each methylene group is usually interpreted as indicating hydrophobicity of the active site. However, we observed that AroAT and DY18 had different dependencies although both enzymes have the same residues in the substrate-binding pocket. For substrates with more than 7 carbons, the aminotransferases did not strictly distinguish between substrates with straight and branched side chains. These results suggest that the recognition of manifold hydrophobic substrates of different shapes might require not only the hydrophobicity of the active site but also enzyme flexibility.

Key words: aromatic amino acid aminotransferase, aspartate aminotransferase, hydrophobic interaction, protein dynamics, substrate specificity.

It has been believed that many enzymes are active against only one kind of substrate. This strict substrate recognition is often observed with hydrogen bonding and ionic interactions (*2*). These electrostatic interactions may be enforced in the interior of the protein due to the hydrophobic environment (*3*). The three-dimensional structures of many hydrophobic-ligand binding proteins suggest the characteristics of the hydrophobic binding mechanism. In many cases, a hydrophobic binding pocket is surrounded by aromatic and aliphatic side chains (*4-6*). However, the detailed mechanism of hydrophobic ligand recognition has not been completely elucidated (*7, 8*). Attempting to engineer hydrophobic substrate and/or ligand specificity is difficult. The conversion of trypsin to chymotrypsin is more complicated than the reverse conversion (*8*). Even when a cavity is observed in a protein, it is difficult to predict whether it will accept a hydrophobic ligand. It has been shown that such cavities can accommodate various ligands with different shapes (*9*). These difficulties may be due to the lack of insight into the dynamic motions of proteins. For the same reason the effect on protein stability of a cavity created by site-directed mutagenesis differs according to the environment around the cavity (*10-12*). Needless to say, protein structures determined by X-ray crystallography or nuclear magnetic resonance imaging are static models. Recently, there have been many attempts to reveal the relationship between the dynamic motion and function of proteins (*13-15*).

In this paper, we describe the dynamic mechanism of recognition of a hydrophobic substrate using aminotransferase as an example. *Escherichia coli* aspartate aminotransferase (L-aspartate:2-oxoglutarate aminotransferase [EC 2.6.1.1] (AspAT) and *E. coli* aromatic amino acid aminotransferase [EC 2.6.1.57] (AroAT) catalyze the

[1] This work was supported in part by Grants-in-Aid for Scientific Research (Nos. 05244101 and 7558224) from the Ministry of Education, Science, Sports and Culture of Japan, and a research grant from the Japan Society for the Promotion of Science ("Research for the Future Program").

[2] Present address: Department of Chemistry, Faculty of Science and Technology, Kinki University, Higashi-Osaka, Osaka 557.

[3] Research Fellow of the Japan Society for the Promotion of Science.

[4] To whom correspondence should be addressed. Tel.: +81-6-850-5433, Fax: +81-6-850-5442, e-mail: kuramitu@bio.sci.osaka-u.ac.jp

Abbreviations: AroAT, *Escherichia coli* aromatic amino acid aminotransferase [EC 2.6.1.57]; AspAT, *E. coli* aspartate aminotransferase [EC 2.6.1.1]; sC*n*, aliphatic amino acid with straight side chain bearing *n* carbon atoms; bC*n*, aliphatic amino acid with branched terminus bearing *n* carbon atoms; DY18, AspAT-AroAT chimeric enzyme whose N-terminal portion before codon 18 is *E. coli* AspAT and C-terminal portion from codon 18 is *E. coli* AroAT; DTNB, [5,5'-dithiobis(2-nitrobenzoic acid)]. The amino acid residues and codons are numbered according to the sequence of porcine cytosolic aspartate aminotransferase (*1*). * indicates the residue supplied by the other subunit of the dimer.

transamination reaction between an amino acid and 2-keto acid *via* the ping-pong bi-bi mechanism (*16-19*). Both are dimeric enzymes composed of identical subunits, each of which binds a cofactor, pyridoxal 5′-phosphate (PLP). AspAT has a high specificity for acidic substrates and weak activity for hydrophobic substrates. AroAT shows high activity for both acidic and hydrophobic substrates (*20*). AspAT and AroAT have 44% amino acid sequence homology, and the residues in the active site are mostly conserved (*1, 21, 22*). These enzymes are unique in being active toward two entirely different kinds of substrates (acidic and hydrophobic substrates). X-ray crystallographic studies of AspAT have revealed its binding site for substrates (*23-26*). The side chain COO^- of a dicarboxylic substrate interacts strongly with the guanidyl group of Arg292*. The side chain of an aromatic substrate occupies the same position as that of the acidic substrate and pushes the Arg292* side chain away towards the solvent environment (*27*).

To elucidate the mechanism of recognition of a hydrophobic substrate, AspAT-AroAT chimeras have been constructed using homologous recombination in *E. coli* cells (*28*). It was confirmed that the spatial structures of the chimeric enzymes were almost the same as those of the wild-type enzymes (*28*). From kinetic studies of chimeric enzymes, it has been suggested that not only residues in the active site but also those distant from the active site contribute to the substrate specificity (*28*).

Kuramitsu *et al.* (*19*) found a linear correlation between the accessible surface area of neutral amino acid substrates and $\Delta G_T^{\ddagger}$, the free energy difference between the unbound enzyme plus substrate (E+S) and the transition state ($ES^{\ddagger}$), but the side chains of the natural amino acid substrates were not uniform. In the present study, we used a series of aliphatic amino acids (*29*) and keto acids with straight and branched side chains, and examined the detailed properties of the hydrophobic-substrate binding pocket.

MATERIALS AND METHODS

Chemicals—The nor-alkyl amino acids $CH_3(CH_2)_{n-3}$-$CH(NH_3^+)COO^-$, where $n=3$ (L-sC3), $n=4$ (L-sC4), $n=5$ (L-sC5), $n=6$ (L-sC6), and $n=8$ (DL-sC8), and the aliphatic amino acids with a branched chain, $(CH_3)_2CH(CH_2)_{n-5}$-$CH(NH_3^+)COO^-$, where $n=5$ (L-bC5) and $n=6$ (L-bC6), were purchased from Sigma (St. Louis). Here "L" denotes L-stereo isomer, while "DL" denotes the mixture of DL-isomers. DL-sC7, DL-sC9, DL-bC7, DL-bC8, and DL-bC9 were synthesized by the acetoamidomalonate method (*30*). The substrates used are listed in Table I. In the calculation of kinetic parameters, the concentration of L-stereo isomer in the mixture of DL-isomers was assumed to be half that of the DL-isomers.

Expression and Purification of Enzymes—The plasmid pKYNH18 overproduces AroAT in *E. coli* TY103 (*aspC, tyrB*, and *recA*) (*31*) under the promoter of the *tyrB* gene encoding AroAT. The expression yield of AroAT under these conditions is lower than that of AspAT expressed under the promoter of the *aspC* gene encoding AspAT (*32*). To obtain a higher yield of AroAT, the coding region of *tyrB* was ligated under the promoter of *aspC* and the first codon of *tyrB* was changed from GTG to ATG using the "homologous ligation" method (*33*). The resulting plasmid, named pUC19GpY, was used to overproduce AroAT in *E. coli* TY103. This plasmid gave as high a yield of AroAT as that of AspAT. AspAT, AroAT and the chimeric enzyme were purified as described previously (*19*).

Pre-Steady-State Kinetic Studies of Half-Transamination Reactions—Aliphatic amino acid substrates with straight and branched side chains were used to estimate the hydrophobic substrate specificities of aminotransferase. For the sC3-sC6 and bC5-bC6 substrates, L-forms were used. For the sC7-sC9 and bC7-bC9 substrates, DL-isoforms were used. The aminotransferases tested here cannot use D-form amino acids as substrates. All measurements were carried out at pH 8.0 and 25°C. The buffer solution contained 50 mM 2-[4-(2-hydroxyethyl)-1-piperazinyl]ethanesulfonic acid (HEPES) with 100 mM KCl and 10 μM EDTA.

The slow reaction was followed spectrophotometrically by monitoring the change in absorption of the bound coenzyme at 360 nm. When the k_{app} value was directly proportional to the substrate concentration, the k_{max}/K_d value was calculated from the equation (*19*)

$$k_{app}=(k_{max}/K_d)\ [S] \quad (1)$$

Thus, the catalytic efficiency, k_{max}/K_d, was given by $k_{app}/[S]$ for these substrates. The rapid reactions were followed using a Union Giken RA-401 stopped-flow spectrophotometer. The reaction curves conformed to a single-exponential process. The free energy differences ($\Delta G_T^{\ddagger}$) between the transition state and unbound enzyme plus substrate for various substrates were calculated using the equation (*19, 34*)

$$\Delta G_T^{\ddagger}=RT\ (\ln(k_B T/h)-\ln(k_{max}/K_d)) \quad (2)$$

where R is the gas constant, T the absolute temperature, k_B the Boltzmann constant, and h the Planck constant.

Stability of Enzymes toward Urea Denaturant—The circular dichroic spectra of enzymes were measured in the presence of various concentrations of urea as a denaturant in a 1-mm cell in the region of 210-250 nm at 25°C. The enzyme concentration was about 0.07 mg/ml. The buffer used contained 5 mM HEPES, 10 mM KCl, and 1 μM EDTA at pH 7.0.

Titration of SH Group of Enzymes—The reaction of SH groups of enzymes with DTNB [5,5′-dithiobis(2-nitrobenzoic acid)] was monitored at 412 nm and 25°C by similar methods to those previously described (*35*). The number of titrated SH groups was calculated using a molar extinction coefficient of nitrothiobenzoate $\varepsilon_M=14{,}100\ M^{-1}\cdot cm^{-1}$ at 412 nm (*36*). The enzyme concentration was about 0.5 mg/ml. The buffer used contained 50 mM HEPES, 100 mM KCl, and 10 μM EDTA at pH 8.0.

Measurement of Amide Proton/Deuterium Exchange—The exchange of hydrogen with deuterium was monitored by Fourier transform infrared spectrophotometry at room temperature. The cell had about 0.1 mm light path length and was composed of CaF_2. At zero time, the enzyme passed through the G-15 column (about 1 ml) equilibrated with D_2O buffer containing 50 mM HEPES, 100 mM KCl, and 10 μM EDTA at pH 8.0. The enzyme concentration was 30-40 mg/ml.

RESULTS

Substrate Specificity—$\Delta G_T^{\ddagger}$, the free energy difference between the unbound enzyme plus substrate (E+S) and the transition state (ES‡), was calculated for various substrates using Eq. 1 or 2. A smaller $\Delta G_T^{\ddagger}$ value indicates higher enzyme activity. In previous studies, $\Delta G_T^{\ddagger}$ values were plotted against the accessible surface area of neutral substrates (*19, 20*). These plots gave approximate lines for AspAT and AroAT but gave scattered points for some substrates.

To standardize the properties of the substrates, we used a series of aliphatic substrates with straight and terminal-branched side chains (Table I). The $\Delta G_T^{\ddagger}$ values were plotted against the number of carbons in the substrate (Fig. 1). The 3-carbon substrates, Ala and pyruvate, whose side chain is a single methyl group, were used as reference substrates for each enzyme. For straight side chain substrates, the activities of AspAT and DY18 for the 4-carbon substrate were lower than those for the 3-carbon substrate. However, AroAT preferred a 4-carbon to a 3-carbon substrate (Fig. 1, a and b). Generally, $\Delta G_T^{\ddagger}$ of all the aminotransferases decreased with an increase in the chain length of the substrate within the range of 4 to 7 carbons (Fig. 1b). The activity of AspAT was maximal for a 7-carbon substrate, whereas those of AroAT and DY18 were maximal for an 8-carbon substrate. AspAT showed lower activities for 8- and 9-carbon substrates than for a 7-carbon substrate (Fig. 1b). These long substrates may be larger than the binding pockets of the enzymes. These results suggest that AroAT and DY18 have larger pockets than AspAT by about one methylene group.

The activities of all three enzymes for branched-terminal substrates increased markedly as the length of the substrate side chain increased from 5 to 9 carbons (Fig. 1, c and

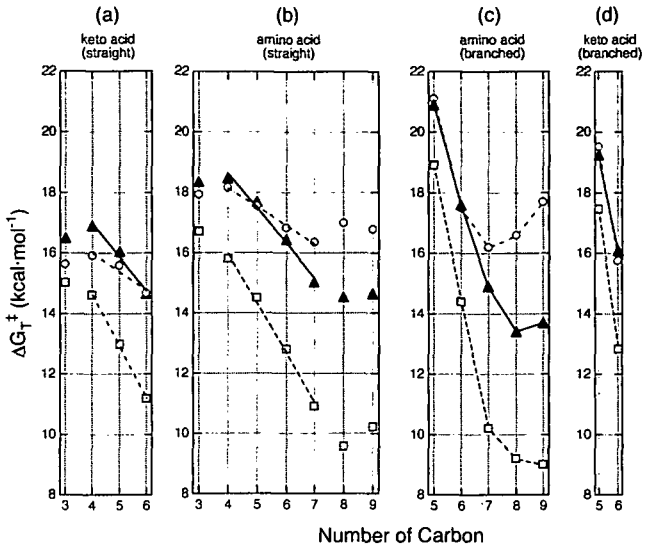

Fig. 1. **Correlation between $\Delta G_T^{\ddagger}$ and the carbon number of the substrate.** ○, AspAT; ▲, DY18; and □, AroAT. $\Delta G_T^{\ddagger}$ is the free energy difference between the unbound enzyme plus substrate (E+S) and the transition state (ES‡) for various amino acid substrates (*34*). $\Delta G_T^{\ddagger}$ was calculated from the k_{max}/K_d value using Eq. 2. The measurements were carried out at pH 8.0, ionic strength 0.1, and 25°C. (a) A series of keto acid substrates with straight side chains. Lines were fitted to the data between 4 and 6. (b) A series of amino acid substrates with straight side chains. Lines were fitted to the data between 4 and 7. (c) A series of amino acid substrates with branched-terminal side chains. (d) A series of keto acid substrates with branched-terminal side chains.

TABLE I. **Side chain structures and kinetic parameters of substrates.**[a]

Side chain	Total carbon	AspAT		AroAT		DY18	
		k_{max}/K_d ($M^{-1}\cdot s^{-1}$)	$\Delta G_T^{\ddagger}$ (kcal·mol^{-1})	k_{max}/K_d ($M^{-1}\cdot s^{-1}$)	$\Delta G_T^{\ddagger}$ (kcal·mol^{-1})	k_{max}/K_d ($M^{-1}\cdot s^{-1}$)	$\Delta G_T^{\ddagger}$ (kcal·mol^{-1})
Amino acid series							
-C	3	0.45	17.9	3.6	16.7	0.22	18.3
-CC	4	0.30	18.2	16	15.8	0.18	18.5
-CCC	5	0.84	17.6	150	14.5	0.67	17.7
-CCCC	6	2.8	16.8	2,600	12.8	5.6	16.4
-CCCCC	7	6.4	16.3	63,000	10.9	59	15.0
-CCCCCC	8	2.2	17.0	600,000	9.6	140	14.5
-CCCCCCC	9	3.1	16.8	200,000	10.2	120	14.6
-C(C)C	5	0.0067	21.1	0.086	18.9	0.0032	20.9
-CC(C)C	6	1.4	17.5	170	14.4	0.75	17.6
-CCC(C)C	7	2.1	16.2	210,000	10.2	74	14.9
-CCCC(C)C	8	4.2	16.6	1,100,000	9.2	930	13.4
-CCCCC(C)C	9	0.66	17.7	1,600,000	9.0	560	13.7
Keto acid series							
-C	3	21	15.6	59	15.0	5.0	16.5
-CC	4	13	15.9	121	14.6	2.6	16.9
-CCC	5	23	15.6	1,900	13.0	11	16.0
-CCCC	6	110	14.7	39,000	11.2	110	14.7
-C(C)C	5	0.030	19.5	0.99	17.5	0.048	19.3
-CC(C)C	6	18	15.7	2,500	12.8	10	16.1

[a]*All measurements were performed in 50 mM HEPES buffer containing 0.1 M KCl at pH 8.0 and 25°C.*

TABLE II. **Positions of cysteine residues.**

Enzyme	Position of cysteine residues				
AspAT[a]	82 (5.8)	191 (7.0)	192 (3.7)	270 (0)	401 (0)
DY18	78	191	192	274	388
AroAT	78	191	192	274	388

[a]Relative accessible surface area (%) to perfectly exposed conformation is shown in parentheses (*24*).

d). Surprisingly, for longer substrates, those with 7 or more carbons, the aminotransferases did not distinguish between straight and branched substrates (compare Fig. 1, b and c). Conversely, the activities for a C_β branched substrate (5 carbons) were markedly lower than for a straight substrate with the same number of carbons.

A keto acid was a better substrate than the corresponding amino acid (Table I). The k_{max}/K_d values for keto acid substrates were 20-30 times greater than those for amino acid substrates. The substrate specificities (slopes for carbon number 4-7) for keto acid substrates were exactly the same as those for amino acid substrates (Fig. 1, a and d). If the geometry of the catalytic group relative to reaction site of substrate is unaltered among each series of amino or keto acid substrates, the k_{max} values should also be unaltered. The fact that the slopes in Fig. 1, a and b, are the same thus means that the affinity between enzyme and aliphatic substrate depends linearly on the carbon number of the substrate.

All three enzymes showed considerable activity toward not only aliphatic substrates but also aromatic substrates. The difference in enzyme activities for aromatic and aliphatic substrates was only about 1-2 kcal/mol, even though the substrates were completely different in shape (*19, 20*).

Flexibility of Enzymes—All three enzymes, AspAT, DY18, and AroAT, have five Cys residues per subunit (Table II). SH groups were titrated with DTNB, and the time courses of the reactions are shown in Fig. 2a. The numbers of SH groups titrated at 180 min were 1, 2, and 3.5 for AspAT, DY18, and AroAT, respectively. The processes of deuterium exchange of amide protons were also measured using infrared spectrophotometry (Fig. 2b). The ratio of amide II/amide I, which shows the extent of deuterium exchange (*37, 38*), increased in the order AspAT, DY18, and AroAT. The stabilities in the presence of urea denaturant also decreased in the same order (Fig. 2c). These experiments indicated that the conformational flexibility increased in the order AspAT, DY18, and AroAT, being consistent with the order of these enzymes in terms of hydrophobic substrate specificity.

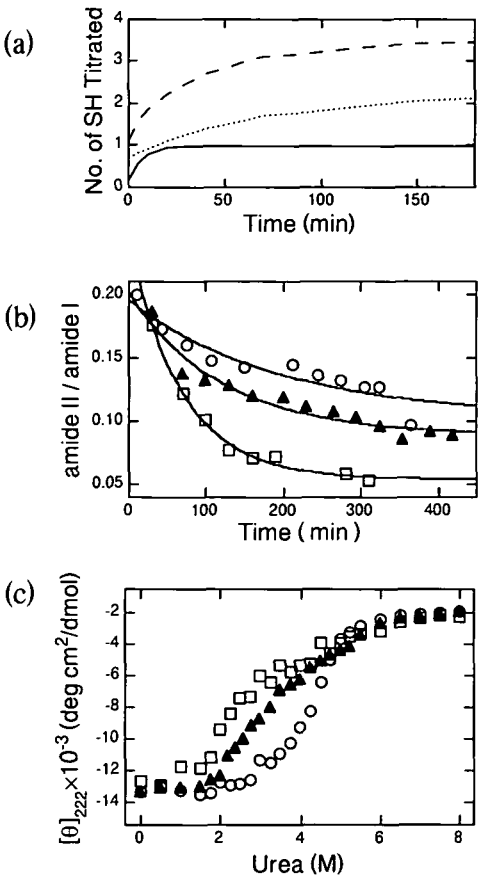

Fig. 2. **Measurements of protein flexibility.** (a) The time course of SH group titration. AspAT (—); DY18 (·····); and AroAT (- - -). (b) The time course of amide proton/deuterium exchange. ○, AspAT; ▲, DY18; and □, AroAT. Vertical axis is the ratio of amide II (1,550 cm^{-1})/amide I (1,650 cm^{-1}). A smaller value shows that more deuterium was exchanged. (c) Stability in the presence of urea denaturant. ○, AspAT; ▲, DY18; and □, AroAT. The values of ellipticity at 222 nm were plotted *versus* the concentration of urea denaturant.

DISCUSSION

The Relationship between Activity and Substrate Carbon Number—The plots of $\Delta G_T^{\ddagger}$ against the accessible surface area of natural amino acid substrates gave straight lines for AspAT and AroAT (*19, 20, 28*). Similarly, when $\Delta G_T^{\ddagger}$ was plotted against the substrate carbon number, the data between 4 and 7 carbons fitted fairly well to straight lines (Fig. 1b). The correlation was better for the series of aliphatic substrates than for natural substrates. The slopes of these lines for amino acid substrates were 1.6, 1.2, and 0.73 kcal·mol^{-1}·CH_2^{-1} for AroAT, DY18, and AspAT, respectively, and the correlation coefficients were 1.00, 0.99, and 1.00, respectively. Although it had not previously been observed (*29*), the use of a 7-carbon substrate enabled us to identify this relationship for AspAT. For keto acid substrates, the corresponding slopes for 4- to 6-carbon substrates were 1.7, 1.1, and 0.62 kcal·mol^{-1}·CH_2^{-1}, respectively, and the correlation coefficients were 1.00, 0.99, and 0.97, respectively (Fig. 1a). By these analyses, we confirmed that the substrate specificities in both directions of the reaction are identical. In the same way, the free energy difference for the transfer of a hydrocarbon from pure liquid to water is proportional to the chain length and the slope is about 0.9 kcal·mol^{-1} (*39*). The linear correlation shown here suggests that the substrate-binding pocket has a considerably uniform and hydrophobic environment, together with substantial conformational freedom. Furthermore, the substrate-binding pockets of AroAT and DY18 may be more hydrophobic than ethanol or dioxane, whereas that of AspAT is less hydrophobic.

The Role of the N-Terminal Region in Hydrophobic Substrate Specificity—The chimeric enzymes we constructed showed no gross conformational changes (*28*). The microenvironments around the coenzyme were also almost

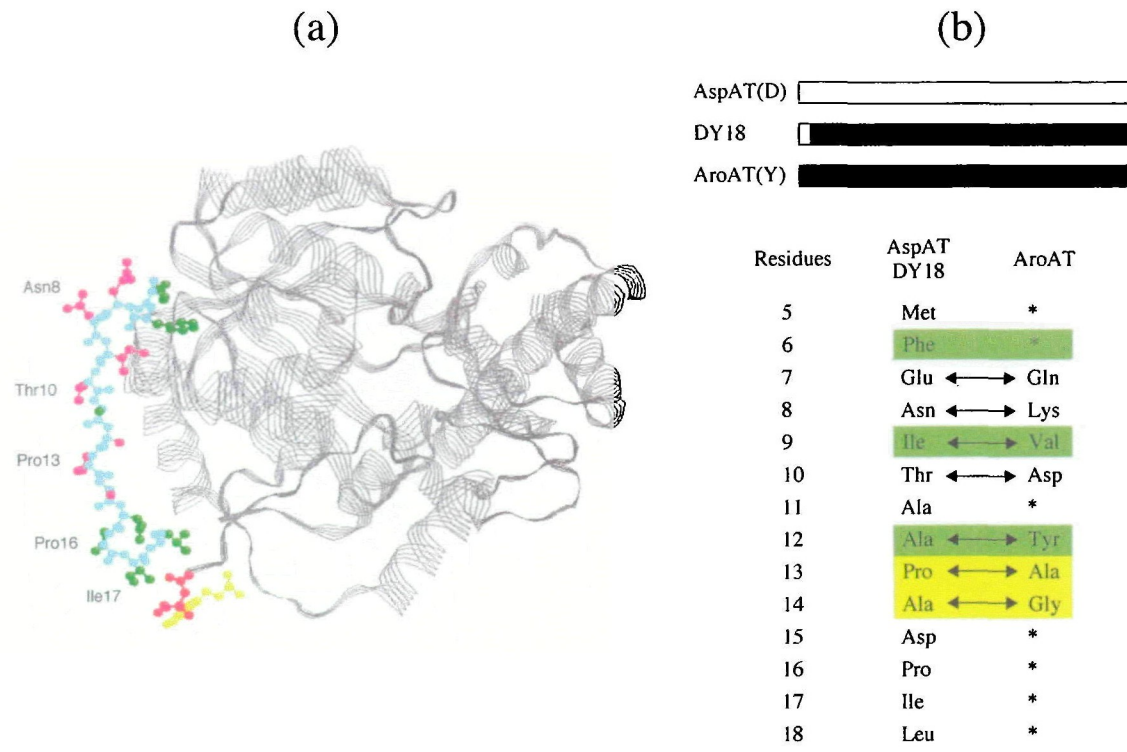

Fig. 3. **Structure of N-terminal portion.** (a) The spatial structure of the N-terminal portion of one subunit (ball and stick model) and another subunit (ribbon model) (*24*). The substrate analogue (red) and cofactor, PLP (yellow), are also shown. (b) Comparison of N-terminal amino acid sequences of AspAT, DY18, and AroAT. Residues 6, 9, and 12 (green) orient to another subunit. Yellow shows Pro-conserved sites in AspAT (see Fig. 4). * shows residues conserved between AspAT and AroAT.

identical to the parental enzymes (*28*). The slopes shown in Fig. 1b have been interpreted to reflect the hydrophobic substrate specificity. Therefore, the slope of DY18 indicates that DY18 was intermediate in specificity between AspAT and AroAT. The hydrophobic substrate specificity of AroAT was greatly altered by mutations in the N-terminal portion. The amino acid residues in the N-terminal regions of AspAT and AroAT are compared in Fig. 3b (*40*). In this region, there are seven mutated residues, that is, DY18 is an AroAT mutant with seven replacements. According to crystallographic studies of AspAT, this N-terminal portion interacts with the large domain of another subunit (Fig. 3a). The side chains of the 6th, 9th and 12th residues orient to that domain (*24*). The 6th residue (Phe) was conserved between AspAT and AroAT. The 9th residue is Ile in AspAT and Val in AroAT, and both have similar properties. The 12th residue is Ala in AspAT and Tyr in AroAT. This 12th residue may interact strongly with the other domain in AroAT. The 13th and 14th residues of AspAT are Pro and Ala, respectively. They are replaced by Ala and Gly, respectively, in AroAT, and these replacements increase the freedom of the polypeptide chain. This region is rich in Pro (1-2 residues) in aspartate aminotransferases (*41-50*), but AroAT has no prolyl residue in this region (Fig. 4). AroAT may have high activities toward hydrophobic substrates through the flexibility of this region. These alterations may contribute to the hydrophobic substrate specificity of aminotransferases. It seems that the replacements (7th, 8th, and 10th residues) do not participate in the substrate specificity because they are far from the active site and their side

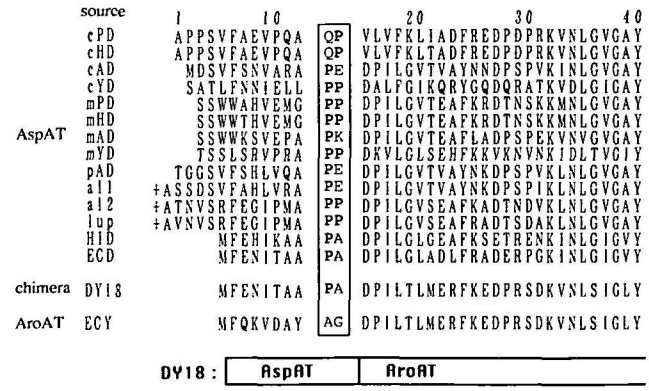

Fig. 4. **Comparison of N-terminal amino acid sequences.** The N-terminal amino acid sequences of 14 different AspATs, DY18, and AroAT are aligned. Pro residue are highly conserved at the 13th and 14th positions of AspAT. At these sites, AroAT has no Pro residues. cPD, cytosolic pig AspAT (*41*); cHD, cytosolic human AspAT (*42*); cAD, cytosolic *Arabidopsis* AspAT (*43*); cYD, cytosolic yeast AspAT (*44*); mPD, mitochondrial pig AspAT (*45*); mHD, mitochondrial human AspAT (*46*); mAD, mitochondrial *Arabidopsis* AspAT (*43*); mYD, mitochondrial yeast AspAT (*47*); pAD, chloroplastic arabidopsis AspAT (*43*); a11, alfalfa AspAT-1 (*48*); a12, alfalfa AspAT-2 (*48*); lup, narrow leaved blue lupine AspAT (*49*); HID, *Haemophilus influenzae* Rd AspAT (*50*); ECD, *Escherichia coli* AspAT (*22*); DY18, chimera between *E. coli* AspAT and AroAT (*28*); and ECY, *E. coli* AroAT (*21*).

chains orient to the outside of the protein (*24*). The above chimera analyses indicate that the N-terminal portion contributes up to about 50% of the hydrophobic substrate

specificity of AroAT, and the other parts may account for the remaining 50% specificity difference.

Mechanism of the Recognition of a Hydrophobic Substrate—The spatial structure of *E. coli* AspAT (*24*) and the amino acid sequences of AspAT and AroAT (*11*) suggest that all residues which directly interact with a substrate are conserved in both enzymes, and that there is no cavity which can accept a large substrate. From our analysis using a series of aliphatic amino acid substrates, the effect of one substrate methyl group was calculated for each carbon position (Fig. 5). Each substrate methyl group uniformly decreased $\Delta G_T^{\ddagger}$ by 1-2 kcal/mol in a wide area of the active site, but not in the vicinity of the substrate β-carbon (Fig. 5). Therefore, we think that the region in the vicinity of the substrate β-carbon is rigid, forming the root of the substrate side chain (the "rigid" region in Fig. 5), and that the interior has a flexible conformation (the "flexible" region in Fig. 5). The latter phenomenon is rarely observed in enzymes with strict substrate specificities. For example, glycyl endopeptidase has a steric barrier to substrates with large side chains (*51*), which is thought to be fixed in the substrate-binding site. Aminoacyl-tRNA synthetases can discriminate between similar amino acid substrates with high precision (*52*). In these cases, flexibility of the binding pocket would be disadvantageous to the strict substrate recognition. Unlike such enzymes, AroAT, AspAT, and DY18 have flexible hydrophobic substrate-binding pockets and may change their conformation according to the bound substrate. Such hydrophobic substrate reorganization of enzymes seems to be ubiquitous, since a linear relationship between substrate hydrophobicity and enzyme activity has been observed for other enzymes (*53-55*).

Relationship between Flexibility and Hydrophobic Substrate Specificity—Numerous studies of amide proton

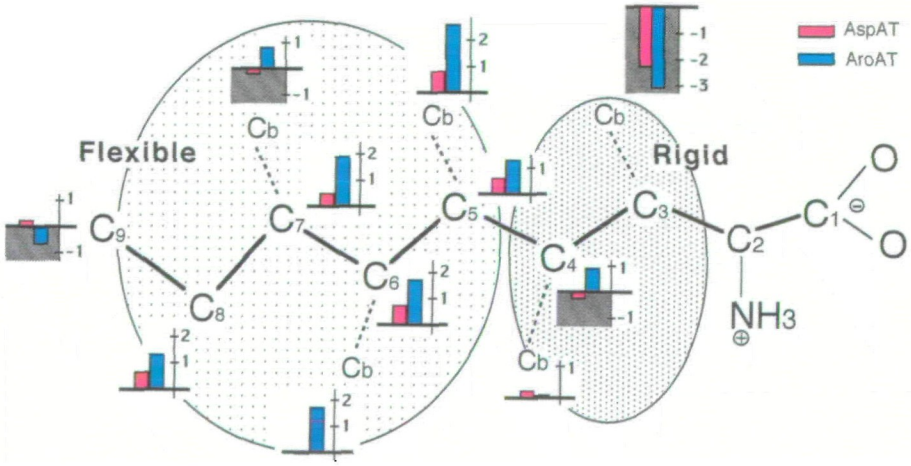

Fig. 5. **The effect of one methyl group of substrate on transition state stabilization.** Red, AspAT; blue, AroAT. Plus value means stabilization and minus value means destabilization of the transition state. The flexible binding subsite and the rigid binding subsite are also shown. These values were calculated for a series of amino acid substrates with straight and branched side chains (Table I). For a keto acid substrates series, similar results were obtained. According to X-ray crystallographic studies (*24*), α-COO^- of substrate is fixed by Arg386. The α-NH_3^+ forms a covalent bond with the aldehyde group of the cofactor, pyridoxal 5′-phosphate. The α-proton of the substrate points to the ε-amino group of Lys258, which is a catalytic group. It is therefore expected that a C_β atom would occupy the same position in all substrates (*64*).

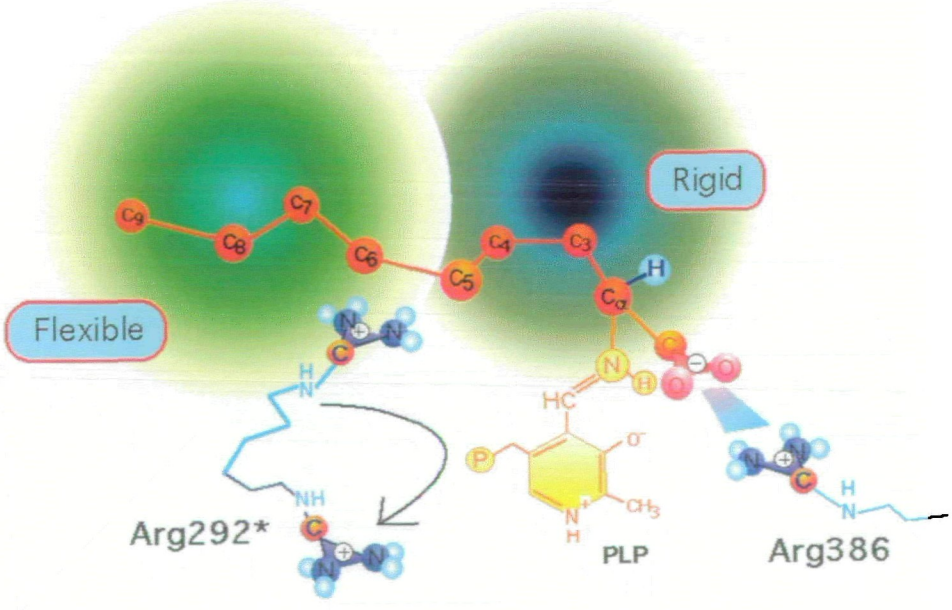

Fig. 6. **Environment of hydrophobic substrate-binding pocket.** Hydrophobic substrate (red) forms an aldimine bond with the cofactor, PLP (yellow). Arg292*, which interacts with the ω-carboxyl group of the dicarboxylic substrate, is pushed away towards the solvent. * shows the residue from another subunit. The vicinity of the β-carbon is rigid (dark blue circle), whereas the interior of the substrate binding pocket is flexible (light blue circle).

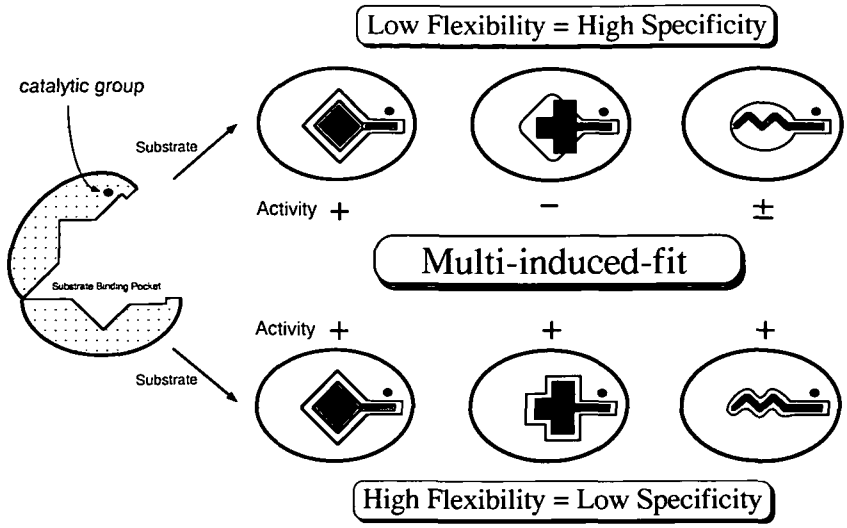

Fig. 7. **Scheme for multi-induced-fit model.** Conformational reorganization of the substrate-binding pocket is induced by each substrate. The upper three cases represent an enzyme with low flexibility and high substrate specificity. The substrate at left is optimal for this enzyme. The lower three cases represent an enzyme with high flexibility and low substrate specificity. The enzyme is able to adapt to all three substrates. This multi-induced-fit model well explains the broad substrate specificity of enzymes that have activities toward various substrates with different shapes.

exchange and aromatic ring motion, using nuclear magnetic resonance, have suggested a correlation between flexibility and protein stability (*56, 57*). The flexibility of the enzymes used here appears to decrease in the order AroAT, DY18, and AspAT, because their ability to exchange an amide proton for deuterium, the sensitivities of their SH groups toward DTNB, and their sensitivity toward urea denaturant decreased in that order (Fig. 2). This order of flexibility is the same as that of hydrophobic substrate specificity. These results may be the first experimental indication that the conformational flexibility of an enzyme contributes to its hydrophobic substrate specificity. The conformational flexibility of the whole enzyme, including the flexibility of the N-terminal region, may enable the enzyme to accept many kinds of substrates. That is, recognition of and/or reactivity toward hydrophobic substrates may require conformational flexibility of the enzyme in order for it to bind multiple substrates. AroAT, AspAT, and DY18 probably have flexible substrate binding pockets that are adjusted to fit the bound substrate. In this case, "flexibility will lead to plasticity"; flexibility refers to a continuum of conformations of almost equal energy, whereas plasticity refers to that conformational changes that occur over an energy barrier of significant height (*58, 59*). Here, we use the term flexibility, because flexibility does not directly relate to plasticity.

As mentioned above, it seems that the binding pocket for a hydrophobic substrate has a uniform hydrophobicity. Here, we should consider the real nature of "hydrophobicity" in the substrate-binding pocket. High hydrophobicity means that there are few water molecules, charged atoms, and polar residues. Alternatively, high packing will make the enzyme-substrate complex stable. The conformational flexibility of the enzyme may contribute to this packing effect during complex formation if the enthalpy change is dominant in the free energy change per methylene group of substrate. AroAT and DY18 have the same sets of residues in the substrate-binding pocket. Therefore, it is reasonable to suggest that AroAT and DY18 have different flexibilities which produce hydrophobic substrate specificity. It has been reported that some proteins have two modes of protein-ligand complexes (*60, 61*). These proteins are expected to have broad energy landscapes (*62, 63*) of the active site conformation.

We propose that conformational reorganization of an enzyme or binding pocket is induced by each bound substrate, particularly hydrophobic substrates of various shapes. The difference in conformational free energy for each enzyme-substrate complex is unexpectedly small. For example, the interior of the substrate binding-pocket seems to be flexible in the aminotransferases used here (Fig. 6). Therefore, conformational flexibility may contribute to substrate specificity. That is, high (or low) flexibility produces an enzyme with a broad (or high) substrate shape specificity (Fig. 7). On the other hand, a high (or broad) specificity for substrate hydrophobicity is promoted by a high (or low) flexibility. These concepts may provide a basis for designing proteins with affinities for hydrophobic ligands. In future, the flexibility and/or plasticity of enzymes should be considered more precisely.

We express our deep gratitude to Dr. Akihiro Okamoto, Osaka Medical Collage, for calculation of the accessible surface area of cystein residues in AspAT and to Mr. Shin-ichi Ishikawa for measurement of IR spectra.

REFERENCES

1. Mehta, P.K., Hale, T.I., and Christen, P. (1989) Evolutionary relationships among aminotransferases. Tyrosine aminotransferase, histidinol-phosphate aminotransferase, and aspartate aminotransferase are homologous proteins. *Eur. J. Biochem.* **186**, 249-253
2. Creighton, T.E. (1993) *Proteins* (2nd ed.) pp. 385-461, W.H. Freeman and Company, New York
3. Fersht, A. (1985) *Enzyme Structure and Mechanism* (2nd ed.) pp. 293-310, W.H. Freeman and Company, New York
4. Xu, Z., Bernlohr, D.A., and Banaszak, L.J. (1993) The adipocyte lipid-binding protein at 1.6-Å resolution. *J. Biol. Chem.* **268**, 7874-7884
5. Kim, J.-J.P., Wang, M., and Paschke, R. (1993) Crystal structures of medium-chain acyl-CoA dehydrogenase from pig liver mitochondria with and without substrate. *Proc. Natl. Acad. Sci. USA* **90**, 7523-7527
6. Winter, N.S., Bratt, J.M., and Banaszak, L.J. (1993) Crystal structures of holo and apo-cellular retinol-binding protein II. *J. Mol. Biol.* **230**, 1247-1259

7. Bone, R., Silen, J.L., and Agard, D.A. (1989) Structural plasticity broadens the specificity of an engineered protease. *Nature* **339**, 191-195
8. Hedstrom, L., Szilagyi, L., and Rutter, W.J. (1992) Converting trypsin to chymotrypsin: The role of surface loops. *Science* **255**, 1249-1253
9. Morton, A., Baase, W.A., and Matthews, B.W. (1995) Energetic origins of specificity of ligand binding in an interior nonpolar cavity of T4 lysozyme. *Biochemistry* **34**, 8564-8575
10. Jackson, S.E., Moracci, M., elMasry, N., Johnson, C.M., and Fersht, A.R. (1993) Effect of cavity-creating mutations in the hydrophobic core of chymotrypsin inhibitor. *Biochemistry* **32**, 11259-11269
11. Serrano, L., Kellis Jr, J.T., Cann, P., Matouschek, A., and Fersht, A.R. (1992) The folding of an enzyme II. Substructure of barnase and the contribution of different interactions to protein stability. *J. Mol. Biol.* **224**, 783-804
12. Eriksson, A.E., Baase, W.A., and Matthews, B.W. (1993) Similar hydrophobic replacements of Leu99 and Phe153 within the core of T4 lysozyme have different structural and thermodynamic consequences. *J. Mol. Biol.* **229**, 747-769
13. Denisov, V.P., Halle, B., Peters, J., and Hörlein, H.D. (1995) Residence times of the buried water molecules in bovine pancreatic trypsin inhibitor and its G36S mutant. *Biochemistry* **34**, 9046-9051
14. Denisov, V.P., Peters, J., Hörlein, H.D., and Halle, B. (1996) Using buried water molecules to explore the energy landscape of proteins. *Nature Struct. Biol.* **3**, 505-509
15. Feher, V.A., Baldwin, E.P., and Dahlquist, F.W. (1996) Access of ligands to cavities within the core of a protein is rapid. *Nature Struct. Biol.* **3**, 516-521
16. Velick, S.F. and Vavra, J. (1962) A kinetic and equilibrium analysis of the glutamic oxaloacetate transaminase mechanism. *J. Biol. Chem.* **237**, 2109-2122
17. Kiick, D.M. and Cook, P.F. (1983) pH studies toward the elucidation of the auxiliary catalyst for pig heart aspartate aminotransferase. *Biochemistry* **22**, 375-382
18. Jenkins, W.T. and Fonda, M.L. (1985) Kinetics, equilibria, and affinity for coenzymes and substrates in *Transaminases* (Christen, P. and Metzler, D.E., eds.) pp. 216-234, John Wiley and Sons, New York
19. Kuramitsu, S., Hiromi, K., Hayashi, H., Morino, Y., and Kagamiyama, H. (1990) Pre-steady-state kinetics of *Escherichia coli* aspartate aminotransferase catalyzed reactions and thermodynamic aspects of its substrate specificity. *Biochemistry* **29**, 5469-5476
20. Hayashi, H., Inoue, K., Nagata, T., Kuramitsu, S., and Kagamiyama, H. (1993) *Escherichia coli* aromatic amino acid aminotransferase: characterization and comparison with aspartate aminotransferase. *Biochemistry* **32**, 12229-12239
21. Kuramitsu, S., Inoue, K., Ogawa, T., Ogawa, H., and Kagamiyama, H. (1985) Aromatic amino acid aminotransferase of *Escherichia coli*: nucleotide sequence of the *tyrB* gene. *Biochem. Biophys. Res. Commun.* **133**, 134-139
22. Kuramitsu, S., Okuno, S., Ogawa, T., Ogawa, H., and Kagamiyama, H. (1985) Aspartate aminotransferase of *Escherichia coli*: nucleotide sequence of the *aspC* gene. *J. Biochem.* **97**, 1259-1262
23. Kamitori, S., Okamoto, A., Hirotsu, K., Higuchi, T., Kuramitsu, S., Kagamiyama, H., Matsuura, Y., and Katsube, Y. (1990) Three-dimensional structures of aspartate aminotransferase from *Escherichia coli* and its mutant enzyme at 2.5 Å resolution. *J. Biochem.* **108**, 175-184
24. Okamoto, A., Higuchi, T., Hirotsu, K., Kuramitsu, S., and Kagamiyama, H. (1994) X-ray crystallographic study of pyridoxal 5′-phosphate-type aspartate aminotransferases from *Escherichia coli* in open and closed form. *J. Biochem.* **116**, 95-107
25. Smith, D., Almo, S., Toney, M., and Ringe, D. (1989) 2.8-Å-resolution crystal structure of an active-site mutant of aspartate aminotransferase from *Escherichia coli*. *Biochemistry* **28**, 8161-8167
26. Danishefsky, A., Onnufer, J., Petsko, G., and Ringe, D. (1991) Activity and structure of the active-site mutants R386Y and R386F of *Escherichia coli* aspartate aminotransferase. *Biochemistry* **30**, 1980-1985
27. Malashkevich, V.N., Onuffer, J.J., Kirsch, J.F., and Jansonius, J.N. (1995) Alternating arginine-modulated substrate specificity in an engineered tyrosine aminotransferase. *Nature Struct. Biol.* **2**, 548-553
28. Miyazawa, K., Kawaguchi, S., Okamoto, A., Kato, R., Ogawa, T., and Kuramitsu, S. (1994) Construction of aminotransferase chimeras and analysis of their substrate specificity. *J. Biochem.* **115**, 568-577
29. Onuffer, J.J., Ton, B.T., Klement, I., and Kirsch, J.F. (1995) The use of natural and unnatural amino acid substrates to define the substrate specificity differences of *Escherichia coli* aspartate and tyrosine aminotransferases. *Protein Sci.* **4**, 1743-1749
30. Barrett, G.C. (1985) *Chemistry and Biochemistry of the Amino Acid*, pp. 246-296, Chapman and Hall, London
31. Yano, T., Kuramitsu, S., Tanase, S., Morino, Y., Hiromi, K., and Kagamiyama, H. (1991) The role of His^{143} in the catalytic mechanism of *Escherichia coli* aspartate aminotransferase. *J. Biol. Chem.* **266**, 6079-6085
32. Kamitori, S., Hirotsu, K., Higuchi, T., Kondo, K., Inoue, K., Kuramitsu, S., Kagamiyama, H., Higuchi, Y., Yasuoka, N., Kusunoki, M., and Matsuura, Y. (1987) Overproduction and preliminary X-ray characterization of aspartate aminotransferase from *Escherichia coli*. *J. Biochem.* **101**, 813-816
33. Kawaguchi, S. and Kuramitsu, S. (1994) Homologous ligation. *Trends Genet.* **10**, 420
34. Fersht, A. (1985) *Enzyme Structure and Mechanism* (2nd ed.), pp. 311-346, W.H. Freeman and Company, New York
35. Kuramitsu, S., Hamaguchi, K., Ogawa, T., and Ogawa, H. (1981) A large-scale preparation and some physicochemical properties of RecA protein. *J. Biochem.* **90**, 1033-1045
36. Riddles, P.W., Blakeley, R.L., and Zerner, B. (1979) Ellman's reagent: 5,5′-dithiobis(2-nitrobenzoic acid)—a reexamination. *Anal. Biochem.* **94**, 75-81
37. Blout, E.R., De Lozé, C., and Asadourian, A. (1961) The deuterium exchange of water-soluble polypeptides and proteins as measured by infrared spectroscopy. *J. Am. Chem. Soc.* **83**, 1895-1900
38. Pfister, K., Kägi, J.H.R., and Christen, P. (1978) Syncatalytic conformational changes in aspartate aminotransferase determined by hydrogen-deuterium exchange. *Proc. Natl. Acad. Sci. USA* **75**, 145-148
39. McAuliffe, C. (1966) Solubility in water of paraffin, cycloparaffin, olefin, acetylene, cycloolefin, and aromatic hydrocarbons. *J. Phys. Chem.* **70**, 1267-1275
40. Mehta, P.K., Hale, T.I., and Christen, P. (1993) Aminotransferases: demonstration of homology and division into evolutionary subgroups. *Eur. J. Biochem.* **214**, 549-561
41. Ovchinnikov, Y.A., Egorov, C.A., Aldanova, N.A., Feigina, M.Y., Lipkin, V.M., Abdulaev, N.G., Grishin, E.V., Kiselev, A.P., Modyanov, N.N., Braunstein, A.E., Polyanovsky, O.L., and Nosikov, V.V. (1973) The complete amino acid sequence of cytoplasmic aspartate aminotransferase. *FEBS Lett.* **29**, 31-34
42. Bousquet-Lemercier, B., Pol, S., Pave-Preux, M., Hanoune, J., and Barouki, R. (1990) Properties of human liver cytosolic aspartate aminotransferase mRNAs generated by alternative polyadenylation site selection. *Biochemistry* **29**, 5293-5299
43. Schultz, C.J. and Coruzzi, G.M. (1995) The aspartate aminotransferase gene family of *Arabidopsis* encodes isoenzymes localized to three distinct subcellular compartments. *Plant J.* **7**, 61-75
44. Cronin, V.B., Maras, B., Barra, D.K., and Doonan, S. (1991) The amino acid sequence of the aspartate aminotransferase from baker's yeast (*Saccharomyces cerevisiae*). *Biochem. J.* **277**, 335-340
45. Kagamiyama, H., Sakakibara, R., Tanase, S., Morino, Y., and Wada, H. (1980) Complete amino acid sequence of mitochondrial aspartate aminotransferase from pig heart muscle. Peptide ordering procedures and the complete sequence. *J. Biol. Chem.* **255**, 6153-6159
46. Martini, F., Angelaccio, S., Barra, D., Pascarella, S., Maras, B.,

Doonan, S., and Bossa, F. (1985) The primary structure of mitochondrial aspartate aminotransferase from human heart. *Biochim. Biophys. Acta* **832**, 46-51
47. Cheret, G., Pallier, C., Valens, M., Daignan-Fornier, B., Fukuhara, H., Bolotin-Fukuhara, M., and Sor, F. (1993) The DNA sequence analysis of the HAP4-LAP4 region on chromosome XI of *Saccharomyces cerevisiae* suggests the presence of a second aspartate aminotransferase gene in yeast. *Yeast* **9**, 1259-1265
48. Gregerson, R.G., Miller, S.S., Petrowski, M., Gantt, J.S., and Vance, C.P. (1994) Genomic structure, expression and evolution of the alfalfa aspartate aminotransferase genes. *Plant Mol. Biol.* **25**, 387-399
49. Reynolds, P.H., Smith, L.A., Dickson, J.M., Jones, W.T., Jones, S.D., Rodber, K.A., Carne, A., and Liddane, C.P. (1992) Molecular cloning of a cDNA encoding aspartate aminotransferase-P2 from lupin root nodules. *Plant Mol. Biol.* **19**, 465-472
50. Fleischmann, R.D., Adams, M.D., White, O., Clayton, R.A., Kirkness, E.F., Kerlavage, A.R., Bult, C.J., Tomb, J.F., Dougherty, B.A., Merrick, J.M., McKenney, K., Sutton, G., FitzHugh, W., Fields, C., Gocayne, J.D., Scott, J., Shirley, R., Liu, L.I., Glodek, A., Kelley, J.M., Weidman, J.F., Phillips, C.A., Spriggs, T., Hedblom, E., Cotton, M.D., Utterback, T.R., Hanna, M.C., Nguyen, D.T., Saudek, D.M., Brandon, R.C., Fine, L.D., Fritchman, J.L., Fuhrmann, J.L., Geoghagen, N.S.M., Gnehm, C.L., McDonald, L.A., Small, K.V., Fraser, C.M., Smith, H.O., and Venter, J.C. (1995) Whole-genome random sequencing and assembly of *Haemophilus influenzae* Rd. *Science* **269**, 496-512
51. O'Hara, B.P., Hemmings, A.M., Buttle, D.J., and Pearl, L.H. (1995) Crystal structure of glycyl endopeptidase from *Carica papaya*: A cysteine endopeptidase of unusual substrate specificity. *Biochemistry* **34**, 13190-13195
52. Fersht, A. (1985) *Enzyme Structure and Mechanism* (2nd ed.), pp. 347-368, W.H. Freeman and Company, New York
53. Wangikar, P.P., Rich, J.O., Clark, D.S., and Dordick, J.S. (1995) Probing enzymatic transition state hydrophobicities. *Biochemistry* **34**, 12302-12310
54. Ryu, K. and Dordick, J.S. (1992) How do organic solvents affect peroxidase structure and function? *Biochemistry* **31**, 2588-2598
55. Dorovska, V.N., Varfolomeyev, S.D., Kazanskaya, N.F., Klyosov, A.A., and Martinek, K. (1972) The influence of the geometric properties of the active centre on the specificity of α-chymotrypsin catalysis. *FEBS Lett.* **23**, 122-124
56. Matthews, S.J., Jandu, S.K., and Leatherbarrow, R.J. (1993) ^{13}C NMR study of the effects of mutation on the tryptophan dynamics in chymotrypsin inhibitor 2: Correlations with structure and stability. *Biochemistry* **32**, 657-662
57. Wüthrich, K., Wagner, G., Richarz, R., and Braun, W. (1980) Correlations between internal mobility and stability of globular proteins. *Biophys. J.* **32**, 549-560
58. Mace, J.E. and Agard, D.A. (1995) Kinetic and structural characterization of mutations of glycine 216 in α-lytic protease: A new target for engineering substrate specificity. *J. Mol. Biol.* **254**, 720-736
59. Mace, J.E., Wilk, B.J., and Agard, D.A. (1995) Functional linkage between the active site of α-lytic protease and distant regions of structure: Scanning alanine mutagenesis of a surface loop affects activity and substrate specificity. *J. Mol. Biol.* **251**, 116-134
60. Lawson, C.L. (1996) An atomic view of the L-tryptophan binding site of *trp* repressor. *Nature Struct. Biol.* **3**, 986-987
61. Loris, R., Maes, D., Poortmans, F., Wyns, L., and Bouckaert, J. (1996) A structure of the complex between concanavalin A and methyl-3,6-di-*O*-(α-D-mannopyranosyl)-α-D-mannopyranoside reveals two binding modes. *J. Biol. Chem.* **271**, 30614-30618
62. Frauenfelder, H., Sligar, S.G., and Wolynes, P.G. (1991) The energy landscapes and motions of proteins. *Science* **254**, 1598-1603
63. Karplus, M. and McCammon, J.A. (1983) Dynamics of proteins: Elements and function. *Annu. Rev. Biochem.* **52**, 263-300
64. Anone, A., Christen, P., Jansonius, J.N., and Metzler, D.E. (1985) Hypothetical mechanism of action of aspartate aminotransferases in *Transaminases* (Christen, P. and Metzler, D.E., eds.) pp. 326-357, John Wiley and Sons, New York